ISET Journal of Earthquake Technology, Paper No. 399, Vol. 37, No. 1-3, March-Sept. 2000, pp. 11-26

SCATTERING AND DIFFRACTION OF SH WAVES ABOVE AN ARBITRARILY SHAPED TUNNEL

Michael E. Manoogian
Department of Civil Engineering and Environmental Science,
Loyola Marymount University,
Los Angeles, California, U.S.A.

ABSTRACT

The weighted residual method was applied to the problem of scattering and diffraction of plane elastic waves, in the form of SH waves, by a tunnel of arbitrary shape located below the surface of a two-dimensional half-space. In order to demonstrate the versatility of the method, it was applied to shallow and deep circular, elliptical, square, and rotated square tunnels with walls that were harder and denser than the surrounding medium. Results obtained were quite similar to those obtained using available closed form solutions. It was shown that significant ground motion amplifications, with respect to the amplitude of incident waves, occurred on the ground surface in the vicinity of the tunnel. Amplifications were dependent upon the shape and depth of the tunnel and the frequency and angle of incidence of incoming SH-waves. Amplification profiles for the lower frequency incident waves were simple near the tunnel on the surface of the half-space with peak amplifications that did not vary much from 2, the value expected on the surface of a smooth half-space in the absence of a sub-surface discontinuity. As the frequency of the incident waves is increased, the amplification profiles near the tunnel became more complicated with peak values exceeding 7 for rotated square shaped tunnels located near the ground surface.

KEYWORDS: Weighted Residuals, SH-Wave, Diffraction, Tunnel, Half-Space

INTRODUCTION

One of the many areas of earthquake engineering and seismological research has been the effect of local site conditions on ground motion. Among the local site topographies of interest are tunnels located below the ground surface. In this paper, the problem of the scattering and diffraction of incident SH waves by an arbitrarily shaped tunnel below the surface of a two-dimensional half-space is studied. A numerical solution for the problem is appropriate as the boundary between the material of the discontinuity and the half-space may be non-circular or irregular, making it difficult to describe the solution in closed form using the cylindrical coordinate system employed. The method of weighted residuals is implemented in order to study possible amplifications and de-amplifications of displacements on the surface of the half-space above and near a sub-surface tunnel.

Currently, with respect to sub-surface discontinuities, closed form solutions exist for a cavity in an infinite space (Pao and Mow, 1973), a circular cavity in a half-space (Lee, 1977), an elastic tunnel and inclusion in a half-space (Lee and Trifunac, 1979), and a circular cavity in a wedge shaped half-space (Lee and Sherif, 1996). With respect to the scattering of SH-waves by surface discontinuities, closed form solutions exist for a semi-cylindrical valley (Trifunac, 1971), a semi-cylindrical canyon (Trifunac, 1973), a semi-elliptical valley (Wong and Trifunac, 1974a), a semi-cylindrical canyon (Wong and Trifunac, 1974b), a circular arc hill (Yuan and Men, 1992), a cylindrical canyon of circular arc cross-section (Yuan and Liao, 1994), a cylindrical alluvial valley of circular arc cross-section (Yuan and Liao, 1995), and a circular alluvial valley in a wedge shaped medium (Sherif and Lee, 1997). Other analytic solutions have been developed by Gregory (1967), Gregory (1970), Datta (1978), Dravinski (1982, 1983). Dravinski (1983) used a boundary integral method to determine the effects of elastic inclusions of arbitrary shape on incident elastic waves in a half-space. A closed form solution for the scattering and diffraction of P, SV, and SH-waves by a three-dimensional alluvial valley has also been developed (Lee, 1984). A closed form solution for the three-dimensional diffraction of elastic waves by a spherical cavity in an elastic half-space was developed by Lee (1988). Datta and El-Akily (1978) and Datta and Shah (1982) used the method of matched wave expansions to address the problem of a cavity buried in elastic

half-space. Datta and Shah (1982), Shah et al. (1982), and Wong et al. (1985) used a hybrid approach combining the finite element method for the medium immediately surrounding the cavity with a wave function expansion or a Green's function representation for the remaining medium. Luco and de Barros (1994a) used an indirect boundary integral approach based on a two dimensional Green's function to determine the seismic response in the vicinity of a cylindrical cavity. Franssens and Lagasse (1984) used a finite element approach to determine the scattering of elastic waves by a cylindrical obstacle embedded in a multi-layered medium. Luco and de Barros (1994b) and de Barros and Luco (1994) used a hybrid approach consisting of an indirect boundary integral based on a moving Green's function for the soil medium and Donnel shell theory for the tunnel wall to determine the seismic response of a cylindrical shell embedded in a half-space. A large body of work has been devoted to the effects of earthquake waves on buried tunnels, pipelines, and other underground structures. A review of this work and bibliography may be found in Luco and de Barros (1994a). Sanchez-Sesma (1987) provides a general review of methods available for the study of site effects on strong ground motion.

This paper presents the application of the weighted residual approach to the scattering and diffraction of incident SH waves by an arbitrarily shaped tunnel below the surface of the half-space. This approach is used to evaluate boundary conditions and is a special case of the method of moments (Harrington; 1967, 1968). This approach has been applied to electromagnetic wave fields (Harrington, 1967), acoustic radiation fields (Fenlon, 1969), scattering and diffraction of SH-waves in a half-space by elastic inclusions, cavities, tunnels, canyons, canals, and alluvial valleys of arbitrary shape (Manoogian, 1992; Manoogian, 1995; Manoogian and Lee, 1995; Lee and Manoogian, 1995; Manoogian, 1996; Manoogian and Lee, 1996; Manoogian, 1998a; Manoogian, 1998b). Manoogian (1998b) is a shorter version of the article presented here. Key differences are a more comprehensive literature review, a demonstration that the weighted residual method results in the equations of the closed form solution for the special case of a circular tunnel in which orthogonality may be assumed, a better set of figures, the additional case of a rotated square tunnel, some further discussion, and some minor additions elsewhere. The method of weighted residuals was used for general elastic waves scattered by canyons of irregular shape (Lee and Wu, 1994a, 1994b) and the scattering of SH-waves by cavities of arbitrary shape in a waveguide (Hayir and Bakyrtaþ, 1999). Use of this method results in a matrix equation from which the unknown coefficients are determined and used to develop a series solution for the scattering, diffraction, and transmission of waves by the tunnel. This paper presents an application of the weighted residual approach used to determine the scattering and diffraction of plane waves by a tunnel of arbitrary shape within an elastic half-space. Boundary conditions for the tunnel differ significantly from those of the cavity and elastic inclusion. The character of amplifications on the ground above tunnels of various shapes are studied. The method is applied to the problem of a tunnel of circular shape in an elastic half-space and compared to closed form solutions in order to verify the approach. Applications to problems of tunnels of other shapes in an elastic half-space are used to show the versatility of the approach. The advantage of the method of weighted residuals addressed in this article with respect to closed form solutions is its versatility. A closed form tunnel solution is limited to a tunnel of specific shape. Once the weighted residual solution is formulated for an arbitrarily shaped tunnel, it may be used for tunnels of various shapes without reformulating the solution.

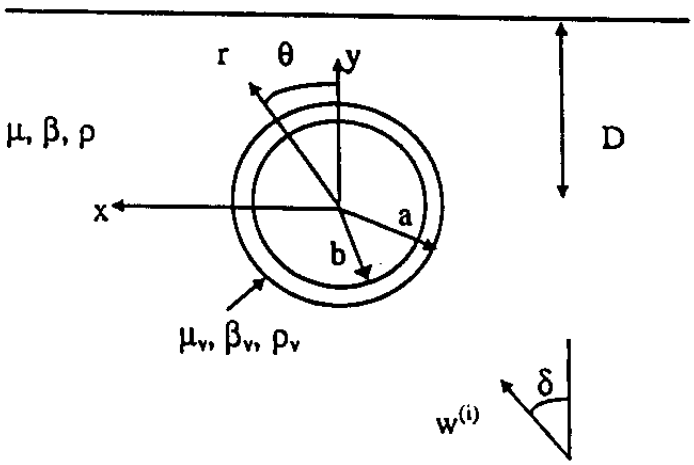

Fig. 1 Tunnel model

MODEL, EXCITATION, AND SOLUTION

The cross section of the model to be studied is shown in Figure 1. It represents a circular tunnel of arbitrary shape situated below the surface of the half-space. Although the approach is derived using a circular tunnel with elastic walls of any thickness t, $0 < t < a$, the resulting equations may be used for a tunnel of any size or shape. Variations from the circular tunnel shape are handled using normal and tangent angles of the tunnel surfaces with respect to the r-axis. The origin is at the center of the tunnel. The half-space is assumed to consist of an elastic, homogeneous, isotropic, material with rigidity μ and shear wave velocity c_β. The material in the tunnel wall is assumed to consist of an elastic, homogeneous isotropic material with rigidity μ_v and shear wave velocity c_{β_v}. Coordinate systems are shown in Figure 1. The z-axis may be assumed to be perpendicular to the plane defined by these coordinate systems.

Initially, define the excitation, $w^{(i)}$, as shown below:

$$w^{(i)} = \exp(-i\omega t)\exp(ikr\cos(\theta - \delta)) \tag{1}$$

This corresponds to a wave with incidence angle δ, amplitude of 1, excitation frequency ω, and wavelength $\lambda = 2\pi / k$, where $k = \omega / c_\beta$, c_x and c_y are the components of the phase velocity in the direction of the coordinate axes. In order to develop a solution to the problem, use the method of imaging (Lee, 1977; Lee and Trifunac, 1979). Consider an unbounded medium with an identical tunnel located at $y = 2D$. Consider two additional coordinate systems defined within the tunnel at O_1 with $(x, y) = (0, 2D)$; a Cartesian coordinate system (x, y_1) and a polar coordinate system (r_1, θ_1) as shown in Figure 2.

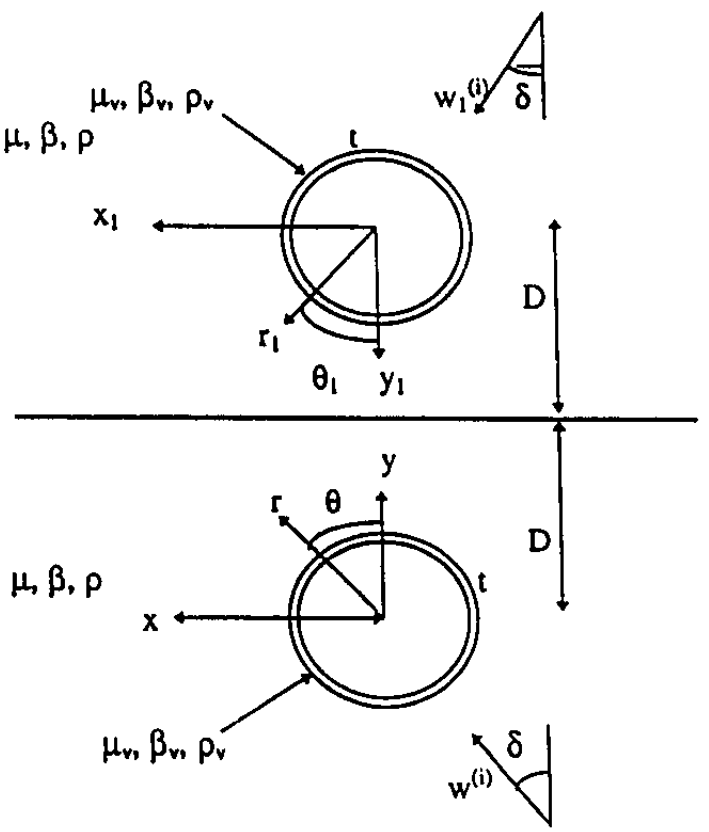

Fig. 2 Tunnel model with image

Assume another incident plane SH-wave as defined below:

$$w_1^{(i)} = \exp(-i\omega t)\exp(ikr_1\cos(\theta_1 - \delta)) \tag{2}$$

Omit $\exp(-i\omega t)$ from latter expressions. Transform $w_1^{(i)}$ into the original coordinate system and combine with $w^{(i)}$ as shown below:

$$w^{(i)} + w_1^{(i)} = \exp(ikr\cos(\theta + \delta)) + \exp(i2kD\cos\delta)\exp(-ikr\cos(\theta - \delta)) \tag{3}$$

Due to the presence of the tunnel, the waves are scattered and diffracted within the half-space and transmitted into the tunnel walls. Practically, a thin tunnel wall would be transparent to longer incident SH-waves. Within the half-space, the result is a sum of the incident, reflected, scattered, and diffracted waves. Within the tunnel, the result consists of the transmitted waves. These must satisfy the wave equation as defined below:

$$\frac{\partial^2 w}{\partial r^2} + \frac{1}{r}\frac{\partial w}{\partial r} + \frac{1}{r^2}\frac{\partial^2 w}{\partial \theta^2} = \frac{1}{c_\beta^2}\frac{\partial^2 w}{\partial t^2} \tag{4}$$

Assume waves scattered by the tunnel and its image in the form shown below:

$$w^{(s)} = \sum_{n=0}^{\infty} H_n^{(1)}(kr)\left(A_n\cos n\theta + B_n\sin n\theta\right) \quad n = 0,1,2,\ldots \tag{5}$$

$$w_1^{(s)} = \sum_{n=0}^{\infty} H_n^{(1)}(kr)\left(A_n\cos n\theta_1 + B_n\sin n\theta_1\right) \quad n = 0,1,2,\ldots \tag{6}$$

Equation (6) is transformed into the (r,θ) coordinate system using the Graf addition theorem (Abramowitz and Stegun, 1964) as given in Lee and Manoogian (1995). Rewrite $w_1^{(s)}$ into the following form

$$w_1^{(s)} = w_1(r,\theta)\sum_{m=0}^{\infty} = J_m(kr)\left(A_m^*\cos m\theta + B_m^*\sin m\theta\right) \tag{7}$$

The transmitted wave, inside the tunnel wall, is defined as shown below:

$$w^{(v)} = \sum_{n=0}^{\infty}[[C_m^{(1)}H_m^{(2)}(k_v r) + C_m^{(2)}H_m^{(1)}(k_v r)]\cos n\theta + [D_m^{(1)}H_m^{(2)}(k_v r) + D_m^{(2)}H_m^{(1)}(k_v r)]\sin n\theta] \tag{8}$$

$$n = 0,1,2,\ldots$$

Define $k_v = \omega/c_\beta$, as the wave number in the tunnel wall. Boundary conditions of interest include the stress free boundary conditions at the free surface of the half-space, displacement and stress continuity conditions at the boundary between the half-space and the tunnel wall, and a stress free condition on the inside face of the wall of the tunnel must be used. The stress free condition at the surface of the half-space is shown below:

$$\tau_{yz} = \mu\frac{\partial w}{\partial y}\Big|_{y=D} = 0 \tag{9}$$

Continuity conditions at the interface between the half-space and the tunnel are shown below:

$$w^{(i)} + w_1^{(i)} + w^{(s)} + w_1^{(s)} = w^{(v)} \tag{10}$$

$$\tau_{nz}^{(i)} + \tau_{1nz}^{(i)} + \tau_{nz}^{(s)} + \tau_{1nz}^{(s)} = \tau_{nz}^{(v)} \tag{11}$$

The stress free boundary condition on the inside wall of the tunnel is shown below.

$$\tau_{nz}^{(v)} = 0 \tag{12}$$

The stress free condition at the surface of the half-space has been met for $w^{(i)}$, $w_1^{(i)}$, $w^{(s)}$, $w_1^{(s)}$ by the method of images. The displacement continuity condition, Equation (10), is satisfied by substituting Equations (3), (5), (7), and (8). Assemble (3), (5), (7), and (8) into Equation (11) in order to satisfy the stress boundary condition. Assemble (8) into (12) in order to satisfy the stress free boundary condition on the rim of the tunnel. Assemble the resulting equations into the weighted residual forms shown below:

$$0 = \int_{\theta_1}^{\theta_N} W_m(r(\theta),\theta)(w^{(i)} + w_1^{(i)} + w^{(s)} + w_1^{(s)} - w^{(v)})d\theta \quad \text{for } m = 0,1,2,... \tag{13}$$

$$0 = \int_{\theta_1}^{\theta_N} W_m(r(\theta),\theta)(\tau^{(i)} + \tau_1^{(i)} + \tau^{(s)} + \tau_1^{(s)} - \tau^{(v)})d\theta \quad \text{for } m = 0,1,2,... \tag{14}$$

$$0 = \int_{\theta_1}^{\theta_N} W_m(r(\theta),\theta)\tau^{(v)}d\theta \quad \text{for } m = 0,1,2,... \tag{15}$$

Define $W_m(r(\theta),\theta)$ as the weight function and $\tau^{(i+r)}$, $\tau^{(s)}$, and $\tau^{(v)}$ as stresses due to the incident and reflected waves, scattered waves, and transmitted waves. The weight functions used in the computations were $\cos m\theta$ and $\sin m\theta$. The number of terms, n and m, used in each solution was based on experimentation for each incident wave frequency, η, for the shallow circular tunnel computations. Sufficient convergence was achieved using a range of $n,m = 0,1,2,3$ for $\eta = 0.25$ and $n,m = 0,1,2,....,12$ for $\eta = 2$. Using the shallow square tunnel solutions for the frequency $\eta = 2$, $\delta = 0^0$ as the worst case example, the surface displacement at $x/a = 0$ was 3.374712, 3.474715, and 3.483500 for maximum values of n and $m = 11,12$ and 13. Tunnels of other shapes as well as deeper square tunnels had smaller differences in displacements as the values of n and m were varied. Weight functions using Bessel and Hankel functions were also tested. Solutions resulting from the use of Hankel functions were successful but resulted in very large coefficients for higher values of n and m in the coefficient matrix, $[C_{mn}]$. It was found that the use of Bessel functions resulted in very small terms for large n and m and in the possibility of an ill conditioned coefficient matrix. The use of $\cos m\theta$ and $\sin m\theta$ as weight functions was sufficient. The weighted residual forms are assembled into matrix form $[C_{mn}]\{\alpha_n\} = \{b_m$ and solved using a Gaussian elimination procedure for complex coefficients. Denote the matrix $[C_{mn}]$ as the matrix of coefficients from Equations (13), (14), and (15). It is a square matrix. Vectors $\{\alpha_n\}$ and $\{b_m\}$ consist of the unknown constants and coefficients from incident and reflected wave weighted residual expressions. Constants A_n, B_n, $C_n^{(1)}$, $C_n^{(2)}$, $D_n^{(1)}$, and $D_n^{(2)}$ are determined and substituted into Equations (5), (7), and (8). The transmitted wave amplitudes are defined by Equation (8). The scattered wave amplitudes are added to Equation (3) to obtain amplitudes in the half-space.

SPECIAL CASE-CIRCULAR UNDERGROUND TUNNEL

The case of a circular tunnel below the surface of an elastic half-space is worthy of special consideration as the closed form analytic solution for incident plane SH waves has been available for almost 20 years (Lee and Trifunac, 1979). Using the (moment) method of weighted residues introduced above, the same continuity equations of displacement and stress can be applied at the surface of the tunnel. Let a and b, respectively, be the outer and inner radius of the tunnel wall with $a > b > 0$. Then the boundary conditions (Equations (9), (10), and (11)) take the following form. At $r = a$, the outer

radius interfacing between the tunnel wall and the half-space, the displacement continuity equation (Equation (10)) stays the same.

$$w^{(i)} + w_1^{(i)} + w^{(s)} + w_1^{(s)} = w^{(v)} \tag{16}$$

The stress continuity equation (Equation (11)) at $r = a$ becomes

$$\mu \frac{\partial}{\partial r}\left(w^{(i)} + w_1^{(i)} + w^{(s)} + w_1^{(s)}\right) = \mu_v \frac{\partial w^{(v)}}{\partial r} \tag{17}$$

with μ and μ_v respectively the shear modulus of the half-space and the medium of the tunnel wall. Similarly, the zero stress condition (Equation (12)) at the inner wall of the tunnel $(r = b)$ becomes

$$\mu_v \frac{\partial w^{(v)}}{\partial r} = 0 \tag{18}$$

In applying the method of weighted residues, Equations (16), (17), (18) may be further simplified using the orthogonality of the sine and cosine functions. Expressions for the incident and reflected plane waves, $w^{(i)}$ and $w_1^{(i)}$, in Equations (1) and (2) may be expanded in terms of Bessel functions (Lee and Manoogian, 1995) in the polar coordinate system with the origin at the center of the tunnel.

$$w^{(i)} = w^{(i)}(r,\theta) = \sum_{m=0}^{\infty} \varepsilon_m i^m J_m(k,r)\left(\cos m\delta \cos m\theta + \sin m\delta \sin m\theta\right) \tag{19}$$

$$w_1^{(i)} = w_1^{(i)}(r,\theta) = \exp(i2kD\cos\delta) \sum_{m=0}^{\infty} \varepsilon_m (-i)^m J_m(k,r)\left(\cos m\delta \cos m\theta - \sin m\delta \sin m\theta\right) \tag{20}$$

Expressions for $w^{(s)}$, $w_1^{(s)}$, and $w^{(v)}$ from Equations (5), (7), and (8) involving the unknown coefficients will be used in the weighted residual equations. This will first be applied at the inner radius $(r = b)$ of the tunnel wall, where the stress is zero. For $m = 0,1,2,\ldots$

$$\mu_r \int_0^{2\pi} \begin{pmatrix} \cos m\theta \\ \sin m\theta \end{pmatrix} \frac{\partial}{\partial r} w^{(v)}|_{r=b}\, d\theta = 0 \tag{21}$$

Here, as before, $\sin m\theta$ and $\cos m\theta$ are the weight functions. At $r = b$, for $m,n = 0,1,2,\ldots$, the stress function $\partial w^{(v)}/\partial r$ from Equation (12) becomes a trigonometric function in θ. The orthogonality of the sine and cosine trigonometric functions may be applied, using the well known identities (Abramowitz and Stegun, 1964)

$$\int_0^{2\pi} \cos m\theta \cos n\theta\, d\theta = \begin{pmatrix} 0 & m \equiv n \\ \pi & m = n \equiv 0 \\ 2\pi & m = n = 0 \end{pmatrix} \tag{22}$$

$$\int_0^{2\pi} \sin m\theta \sin n\theta\, d\theta = \begin{pmatrix} 0 & m \equiv n \\ \pi & m = n \equiv 0 \\ 0 & m = n = 0 \end{pmatrix} \tag{23}$$

and

$$\int_0^{2\pi} \cos m\theta \sin n\theta d\theta = 0 \quad \text{for any } m,n \tag{24}$$

resulting, for $m = 0,1,2,...$

$$\begin{aligned} C_m^{(1)} H_m^{(1)'}(k_v b) + C_m^{(2)} H_m^{(2)'}(k_v b) = 0 \\ D_m^{(1)} H_m^{(1)'}(k_v b) + D_m^{(2)} H_m^{(2)'}(k_v b) = 0 \end{aligned} \tag{25}$$

where $H_m^{(1)'}$ and $H_m^{(2)'}$ are the derivatives of $H_m^{(1)}$ and $H_m^{(2)}$. Equation (25) enables $C_m^{(2)}$ and $D_m^{(2)}$ to be expressed in terms of $C_m^{(1)}$ and $D_m^{(1)}$ respectively for each m. Next, the weighted residues integral for the displacement continuity at $r = a$ takes the form for $m = 0,1,2,...$

$$\int_0^{2\pi} \begin{pmatrix} \cos m\theta \\ \sin m\theta \end{pmatrix} (w^{(i)} + w_1^{(i)} + w^{(s)} + w_1^{(s)} - w^{(v)})|_{r=a} d\theta = 0 \tag{26}$$

Again, the orthogonality of the sines and cosines gives, for $m = 0,1,2,...$

$$\begin{aligned} A_m \frac{H_m^{(1)}(ka)}{J_m(ka)} + A_m^* + \varepsilon_m i^m \cos m\delta (1 + (-1)^m e^{i2kD\cos\delta}) \\ - \frac{C_m^{(1)} H_m^{(1)}(k_v a) + C_m^{(2)} H_m^{(2)}(k_v a)}{J_m(ka)} = 0 \end{aligned} \tag{27}$$

and

$$\begin{aligned} B_m \frac{H_m^{(1)}(ka)}{J_m(ka)} + B_m^* + \varepsilon_m i^m \cos m\delta (1 - (-1)^m e^{i2kD\cos\delta}) \\ - \frac{D_m^{(1)} H_m^{(1)}(k_v a) + D_m^{(2)} H_m^{(2)}(k_v a)}{J_m(ka)} = 0 \end{aligned} \tag{28}$$

Similarly, the orthogonality property for the stress continuity equation gives at $r = a$ for $m = 0,1,2,...$

$$\int_0^{2\pi} \begin{pmatrix} \cos m\theta \\ \sin m\theta \end{pmatrix} \frac{\partial}{\partial r} (w^{(i)} + w_1^{(i)} + w^{(s)} + w_1^{(s)} - \frac{\mu_v}{\mu} w^{(v)})|_{r=a} d\theta = 0 \tag{29}$$

The following equations result

$$\begin{aligned} A_m \frac{H_m^{(1)'}(ka)}{J_m'(ka)} + A_m^* + \varepsilon_m i^m \cos m\delta (1 + (-1)^m e^{i2kD\cos\delta}) \\ - (\frac{\mu_v}{\mu})(\frac{k_v}{k}) \frac{C_m^{(1)} H_m^{(1)'}(k_v a) + C_m^{(2)} H_m^{(2)'}(k_v a)}{J_m'(ka)} = 0 \end{aligned} \tag{30}$$

$$B_m \frac{H_m^{(1)'}(ka)}{J_m'(ka)} + B_m^* + \varepsilon_m i^m \cos m\delta (1-(-1)^m e^{(2kD\cos\delta)}) - (\frac{\mu_v}{\mu})(\frac{k_v}{k}) \frac{D_m^{(1)} H_m^{(1)'}(k_v a) + D_m^{(2)} H_m^{(2)'}(k_v a)}{J_m'(ka)} = 0 \quad (31)$$

with $H_m^{(1)'(2)'}(.)$, and $J_m'(.)$ denoting respectively the first order derivatives of the corresponding Hankel and Bessel functions.

The expressions for the coefficients for $m = 0, 1, 2, \ldots$ in the above are of the same form as the analytic closed form expressions derived earlier (Lee and Trifunac, 1979) in solving the diffraction problem of a circular underground tunnel as a boundary value problem using wave propagation theory. By comparing the resulting displacement amplitudes calculated using the exact analytic approach earlier and the weighted residue approach used here as a numerical method, the validity of the approximate numerical method can be tested and improved upon. The residual method can be applied with confidence to problems involving other arbitrarily shaped tunnels when analytic solutions are not available.

SURFACE DISPLACEMENTS

Of particular interest are the displacement amplitudes on the surface of the half-space above the tunnel. If the amplitude of the incident plane SH-waves is 1, the responses shown define amplification and de-amplification factors. The resultant motion is defined by the modulus, $amplitude = (Re^2(w) + Im^2(w))^{1/2}$. In the absence of the tunnel, for a uniform half-space, the modulus of the ground displacement is 2 (Achenbach, 1973). Due to the existence of the tunnel, incident waves are scattered and diffracted into the half-space and transmitted into the tunnel, and moduli differ significantly from 2. Displacements were calculated for a discrete set of dimensionless frequencies at intervals of 0.25 ranging from 0.25 to 2. The dimensionless frequency is $\eta = 2a/\lambda = ka/\pi = \omega a/\pi\beta$, with a representing the radius of the tunnel, based on the properties of the half-space. Figures that follow show the displacement amplitudes on the surface of the half-space. All displacements are plotted with respect to the dimensionless distance x/a for incident waves of unit amplitude. Results that follow are based on tunnels with stiffer and denser walls, with properties similar to those used in Lee and Trifunac (1979). Results for circular tunnels were visually compared to those for similarly situated and configured tunnels of Lee and Trifunac (1979), the benchmark closed form solution used by others such as de Barros and Luco (1994). As a result of the selected properties and the practical thickness of the tunnel walls, SH-waves are predominantly scattered into the half-space.

Figure 3 shows the surface displacement amplitudes for the case of a circular tunnel for a frequency range from 0.25 to 2 for an incident wave with an angle of incidence of 0^0, $\mu_v/\mu = 3$, $\rho_v/\rho = 3$, $D = 1.5a$, $t = 0.1a$. Figure 4 shows the surface displacement amplitudes for the same tunnel for a frequency $\eta = 2$ and angles of incidence of 0°, 30°, 60°, and 90°. Amplitude profiles on the half-space become more prominent and complex for higher frequency incoming waves. For lower frequency incoming SH-waves, the amplitudes are smoother and tend towards 2. Amplitudes for vertically incident waves are symmetrical with respect to $x/a = 0$. The largest amplitude was 4.05 for a frequency of $\eta = 2$. Laterally incident waves for $x/a < 0$ result in amplitude profiles that are complicated with higher, sharper peaks. At $x/a > 0$, a shadow zone exists with simpler amplitude profiles with values closer to 2. Solutions for this case are similar by visual comparison to Figure 6 of Lee and Trifunac (1979).

Figure 5 shows the surface displacement amplitudes for the case of a deeper circular tunnel for a frequency range from 0.25 to 2 for an incident wave with an angle of incidence of 60^0, $\mu_v/\mu = 3$, $\rho_v/\rho = 3$, $D = 5a$, $t = 0.1a$. Figure 6 shows the surface displacement amplitudes for the same tunnel for a frequency $\eta = 2$ and angles of incidence of 0°, 30°, 60°, and 90°. Amplitude profiles on the half-space are similar in character but less prominent than for those for the shallower

tunnels of Figures 3 and 4. The largest amplitude was 2.95 for a frequency of $\eta = 2$. Solutions for this case again are similar to those given in Figure 4 of Lee and Trifunac (1979).

Figure 7 shows the surface displacement amplitudes above an elliptical tunnel with $b/a = 0.75$ where b is the minor radius of the tunnel, $D = 1.5a, \delta = 30^0$, $\mu_v/\mu = 3$, and $\rho_v/\rho = 3$, $t = 0.1a$. Figure 8 shows the surface displacement amplitudes for the same tunnel for a frequency $\eta = 2$ and angles of incidence of 0°, 30°, 60°, and 90°. Lower frequency incident waves produce simple surface amplification profiles. Higher frequency incident waves result in amplification profiles, which are more complex with higher peak values. The largest amplitude was 5.10 for an angle of incidence of 90° and a frequency of $\eta = 2$. Laterally incident waves for $x/a < 0$ result in amplitude profiles that are complicated with higher, sharper peaks. At $x/a > 0$, a shadow zone exists with simpler amplitude profiles with values closer to 2. For vertically incident waves, amplitude profiles are symmetrical.

Figure 9 shows the surface displacement amplitudes for a shallow square tunnel with, $D = 1.5a$, where $2a$ is the width of the tunnel, $\delta = 60^0, \mu_v/\mu = 3$, and $\rho_v/\rho = 3$, $t = 0.1a$. Figure 10 shows the surface displacement amplitudes for the same tunnel for a frequency $\eta = 2$ and angles of incidence of 0°, 30°, 60°, and 90°. For laterally incident waves, amplification profiles on the half-space are more prominent and complex for $x/a < 0$ with higher peak amplitudes. On the other side of the tunnel, $x/a > 0$, the amplitude profiles are smoother and tend towards 2. For vertically incident waves, amplitude profiles are symmetrical. The largest amplitude was 5.03 for an angle of incidence of 90° and a frequency of $\eta = 2$.

Figure 11 shows the surface displacement amplitudes for the case of a rotated square tunnel for a frequency range from 0.25 to 2 for an incident wave with an angle of incidence of 90^0, $\mu_v/\mu = 3$, $\rho_v/\rho = 3$, $D = 1.5a$, $t = 0.1a$. Figure 12 shows the surface displacement amplitudes for the same tunnel for a frequency $\eta = 2$ and angles of incidence of 0°, 30°, 60°, and 90°. For laterally incident waves, amplitude profiles on the half-space become more prominent and complex with higher peak values for $x/a < 0$. On the other side of the tunnel, $x/a > 0$, the amplitude profiles are smoother and tend towards 2. For vertically incident waves, amplitude profiles are symmetrical. The largest amplitude was 7.49 for an angle of incidence of 0° and a frequency of $\eta = 2$. Solutions for this case match with those obtained in Lee and Trifunac (1979).

In general, surface displacements as a result of lower frequency incident waves are simple and vary slightly from 2 as the tunnel is nearly transparent to these waves. As the incident wave frequency is increased, the wavelength of the incident wave is closer to the tunnel diameter, and resulting surface displacements are more complex with values significantly larger than 2. High amplitudes are due to the development of standing waves between the upper surface of the tunnel and the surface of the half-space.

CONCLUSIONS

1. The weighted residual approach approximation for the scattering, diffraction, and transmission of SH-waves by a tunnel yields solutions, which closely resemble the known closed form solutions.
2. The weighted residual method is another useful method that may be used to determine the effects of scattering and diffraction of incident SH-waves for tunnels of circular as well as non-circular shapes.
3. Ground surface amplitudes on the half-space above the tunnel may be significantly larger than 2 for a homogeneous half-space. Amplitudes depend on the angle of incidence and frequency of the incoming wave, the shape and depth of the tunnel. These computed amplifications indicate that the presence of an underground tunnel may result in the amplification of earthquake waves.

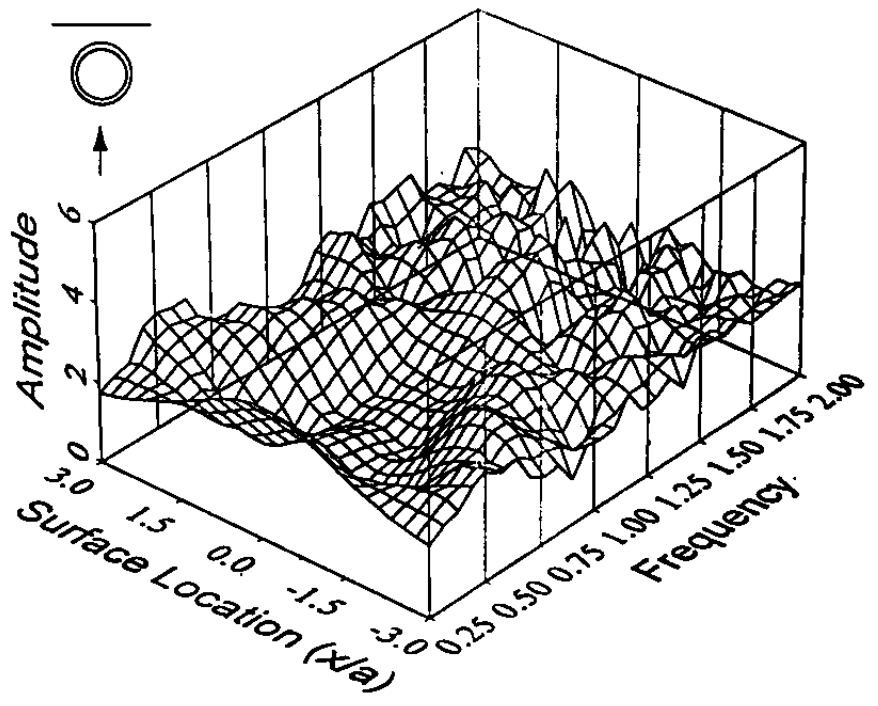

Fig. 3 Amplitudes on the surface of the half-space above a circular tunnel for an incident SH-wave, $\delta = 0^0$, $\mu_v/\mu = 3$, $\rho_v/\rho = 3$, $D = 1.5a$, $t = 0.1a$

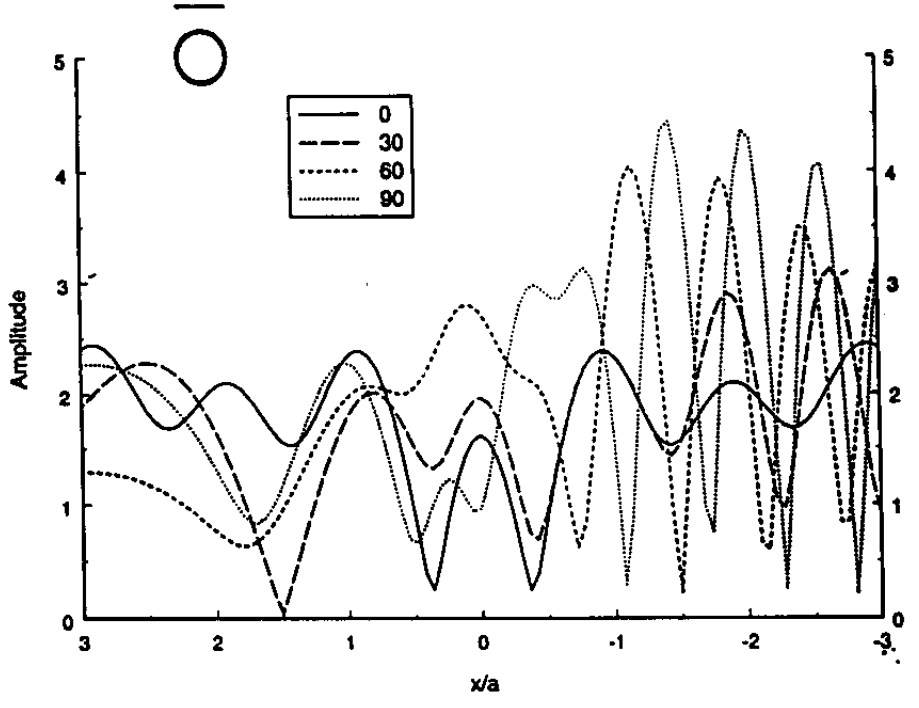

Fig. 4 Amplitudes on the surface of the half-space above a shallow circular tunnel for various angles of incidence, $\mu_v/\mu = 3$, $\rho_v/\rho = 3$, $D = 1.5a$, $t = 0.1a$

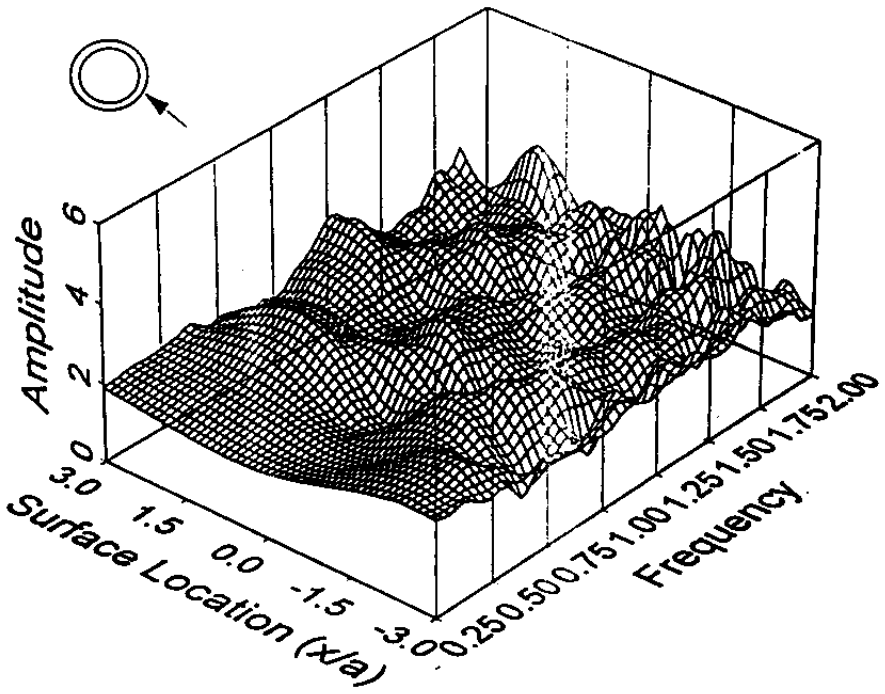

Fig. 5 Amplitudes on the surface of the half-space above a circular tunnel for an incident SH-wave, $\delta = 60^0$, $\mu_v/\mu = 3$, $\rho_v/\rho = 3$, $D = 5a$, $t = 0.1a$

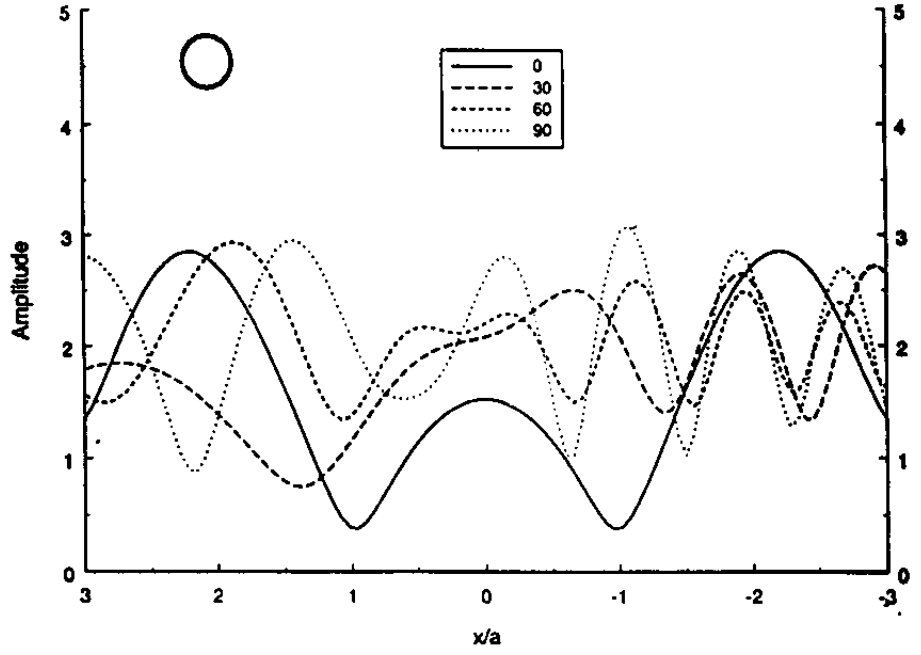

Fig. 6 Amplitudes on the surface of the half-space above a deep circular tunnel for various angles of incidence, $\mu_v/\mu = 3$, $\rho_v/\rho = 3$, $D = 1.5a$, $t = 0.1a$

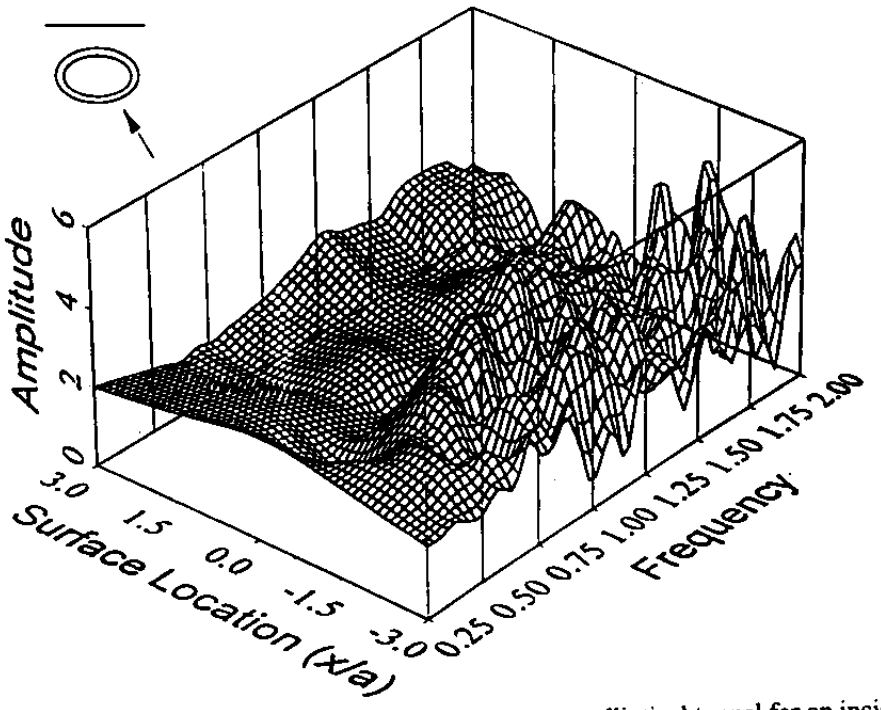

Fig. 7 Amplitudes on the surface of the half-space above an elliptical tunnel for an incident SH-wave, $\delta = 30^0$, $b/a = 0.75$, $D = 1.5a$, $\delta = 30^0$, $\mu_v/\mu = 3$, $\rho_v/\rho = 3$, $t = 0.1a$

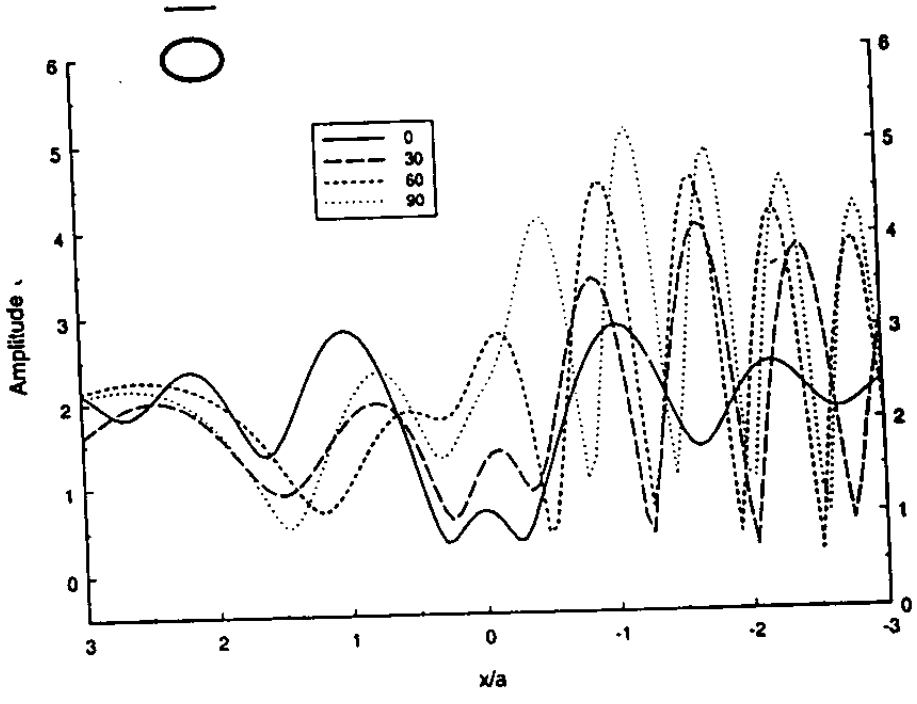

Fig. 8 Amplitudes on the surface of the half-space above a shallow elliptical tunnel for various angles of incidence, $\mu_v/\mu = 3$, $\rho_v/\rho = 3$, $D = 1.5a$, $t = 0.1a$

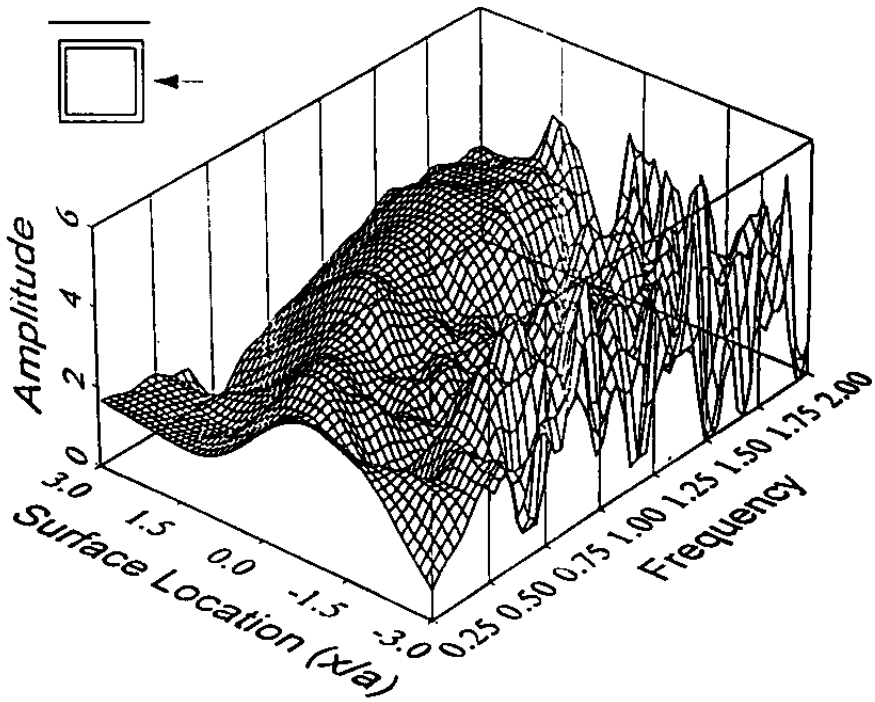

Fig. 9 Amplitudes on the surface of the half-space above a square tunnel for an incident SH-wave, $\delta = 90^{\circ}$, $\mu_v/\mu = 3$, $\rho_v/\rho = 3$, $D = 1.5a$, $t = 0.1a$

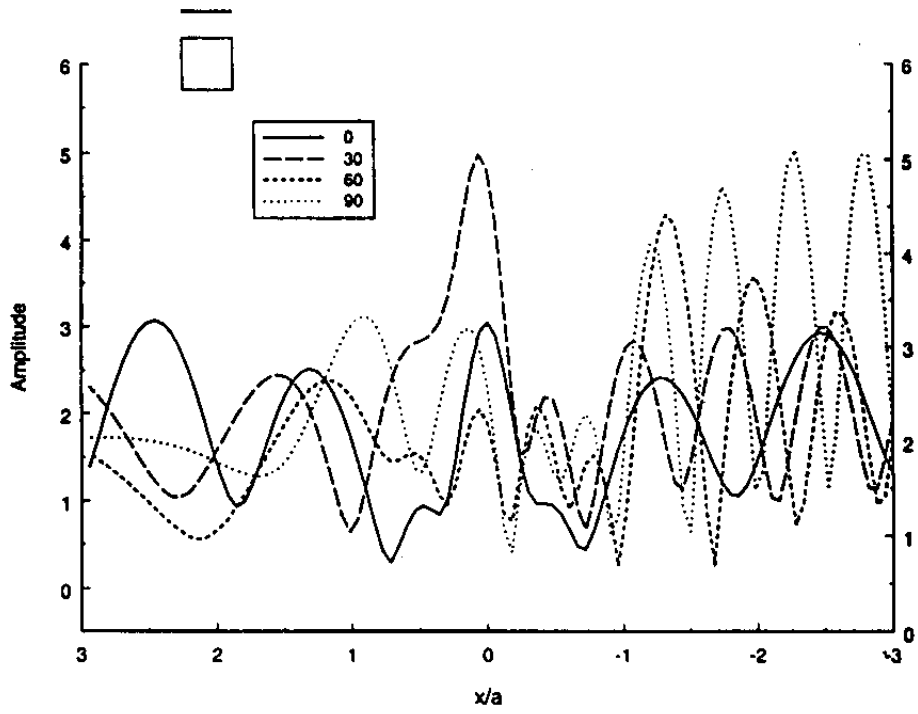

Fig. 10 Amplitudes on the surface of the half-space above a shallow square tunnel for various angles of incidence, $\mu_v/\mu = 3$, $\rho_v/\rho = 3$, $D = 1.5a$, $t = 0.1a$

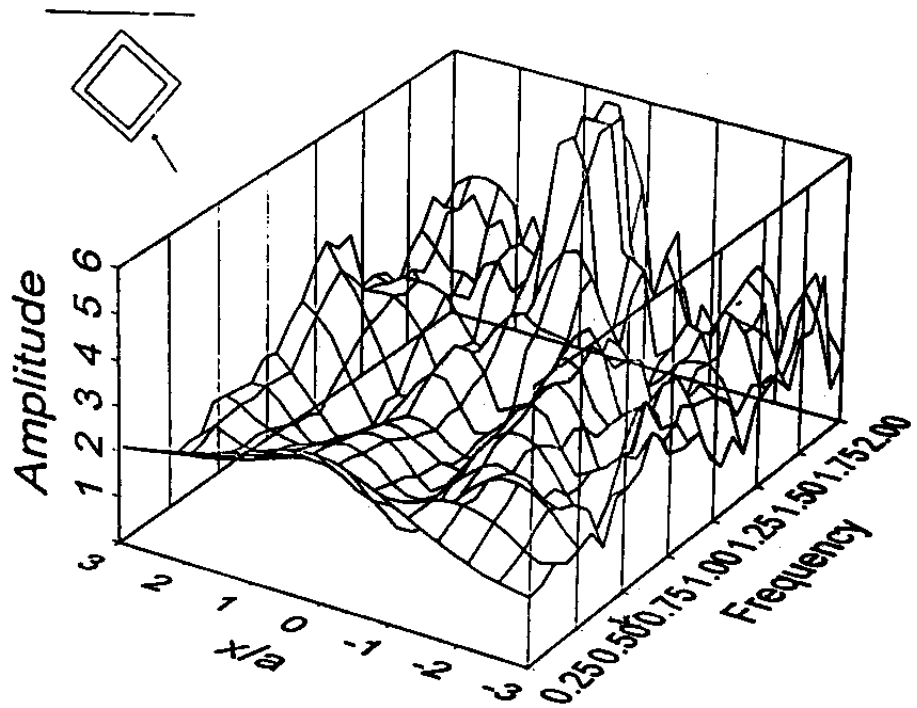

Fig. 11 Amplitudes on the surface of the half-space above a rotated square tunnel for an incident SH-wave, $\delta = 30^0$, $\mu_v/\mu = 3$, $\rho_v/\rho = 3$, $D = 1.5a$, $t = 0.1a$

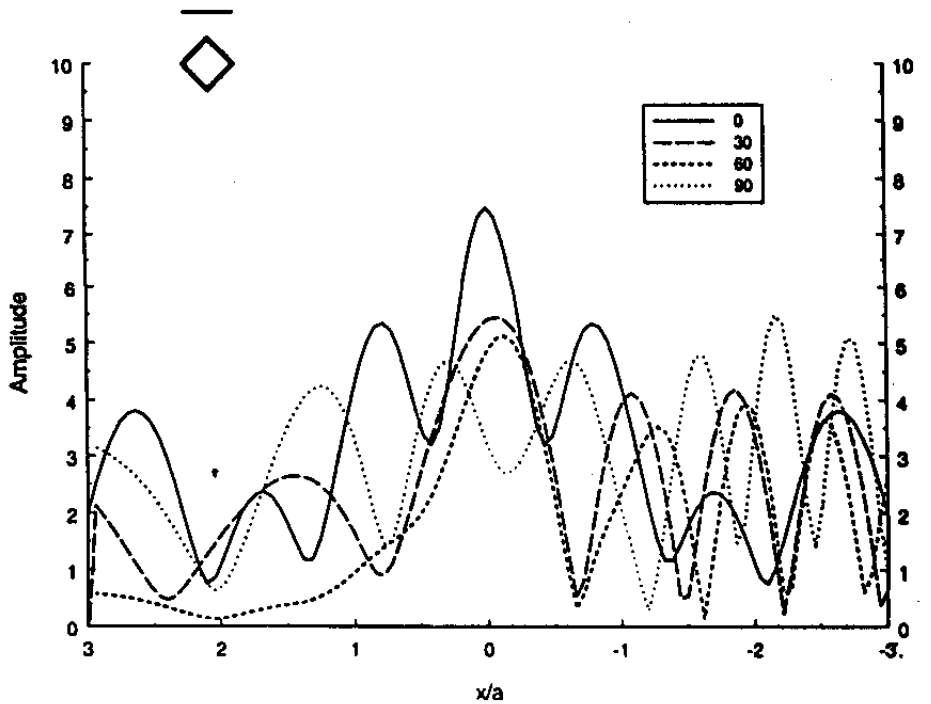

Fig. 12 Amplitudes on the surface of the half-space above a shallow rotated square tunnel for various angles of incidence, $\mu_v/\mu = 3$, $\rho_v/\rho = 3$, $D = 1.5a$, $t = 0.1a$

REFERENCES

1. Abramowitz, M. and Stegun, I.A. (1972). "Handbook of Mathematical Functions, with Formulas, Graphs, and Mathematical Tables", Dover 0-486-61272-4, New York, U.S.A.
2. Achenbach, J.D. (1973). "Wave Propagation in Elastic Solids", North-Holland Publishing Company, Amsterdam, The Netherlands.
3. Datta, S.K. (1978). "Scattering of Elastic Waves", Mechanics Today, Vol. 4, pp. 149-208.
4. Datta, S.K. and Shah, A.H. (1982). "Scattering of SH-Waves by Embedded Cavities", Wave Motion, Vol. 4, pp. 265-283.
5. Datta, S.K. and El-Akily, N. (1978). "Diffraction of Elastic Waves by a Cylindrical Cavity in a Half-Space", J. Acoust. Soc. Am., Vol. 64, pp. 1692-1699.
6. de Barros, F.C.P. and Luco, J.E. (1994). "Seismic Response of a Cylindrical Shell Embedded in a Layered Viscoelastic Half-Space: I. Numerical Results", Earthquake Eng. Struct.. Dyn., Vol. 23, pp. 569-580.
7. Dravinski, M. (1982). "Scattering of SH-Waves by Sub-Surface Topography", ASCE Eng. Mech. Div., Vol. 108, pp. 1-17.
8. Dravinski, M. (1983). "Ground Motion Amplification due to Elastic Inclusions in a Half-Space", Earthquake Eng. Struct. Dyn., Vol. 11, pp. 313-335.
9. Fenlon, F.H. (1969). "Calculation of the Acoustic Radiation Field at the Surface of a Finite Cylinder by the Method of Weighted Residuals", Proceedings of IEEE, Vol. 57, No. 3, pp. 291-306.
10. Franssens, G.R. and Lagasse, P.E. (1984). "Scattering of Elastic Waves by a Cylindrical Obstacle in a Multilayered Medium", J. Acoust. Soc. Am., Vol. 76, pp. 1535-1541.
11. Gregory, R.D. (1967). "An Expansion Theorem Applicable to Problems of Wave Propagation in an Elastic Half-Space", Proc. Camb. Philos. Soc., Vol. 63, pp. 1341-1367.
12. Gregory, R.D. (1970). "The Propagation of Waves in an Elastic Half-Space Containing a Circular Cylindrical Cavity", Proc. Camb. Philos. Soc., Vol. 67, pp. 689-710.
13. Harrington, R.F. (1967). "Matrix Methods for Field Problems", Proceedings of IEEE, Vol. 55, No. 2, pp. 136-149.
14. Harrington, R.F. (1968). "Field Computation by Method of Moments", The MacMillan Company, New York, U.S.A.
15. Hayir, A. and Bakýrtaþ, Y. (1999). "Scattering of SH-Waves by Cavities of Arbitrary Shape in a Waveguide", 13th ASCE Eng. Mech. Conf., Baltimore, Maryland, USA.
16. Lee, V.W. (1977). "On Deformations near a Circular Underground Cavity Subjected to Incident Plane SH-Waves", Proceedings of the Application of Computer Methods in Engineering Conference, Vol. II, University of Southern California, Los Angeles, Calif., U.S.A., pp. 951-962.
17. Lee, V.W. (1984). "Three Dimensional Diffraction of Plane P, SV and SH-Waves by a Hemispherical Alluvial Valley", Soil Dyn. Earthquake Eng., Vol. 3, No. 3, pp. 133-144.
18. Lee, V.W. (1988). "Three Dimensional Diffraction of Elastic Waves by a Spherical Cavity in an Elastic Half-Space I: Closed-Form Solutions", Soil Dyn. and Earthquake Eng., Vol. 7, pp. 149-161.
19. Lee, V.W. and Manoogian, M.E. (1995). "Surface Motion above an Arbitrarily Shaped Underground Cavity for Incident SH-Waves", J. of European Association for Earthquake Eng., Vol. 8, pp. 3-11.
20. Lee, V.W. and Sherif, R. (1996). "Diffraction of Circular Canyons by SH-waves in a Wedge Shaped Half-Space: Analytic Solutions", ASCE Eng. Mech. Div., Vol. 122, pp. 539-544.
21. Lee, V.W. and Trifunac, M.D. (1979). "Response of Tunnels to Incident SH-Waves", ASCE Engg. Mech. Div, Vol. 105, pp. 643-659.
22. Lee, V.W. and Wu, X. (1994a). "Application of the Weighted Residues (Moment) Method to Scattering by 2-D Canyons of Arbitrary Shape: I. Incident SH-Waves", Soil Dyn. Earthquake Eng., Vol. 13, pp. 355-364.

23. Lee, V.W. and Wu, X. (1994b). "Application of the Weighted Residues (Moment) Method to Scattering by 2-D Canyons of Arbitrary Shape: II. Incident P, SV, and Rayleigh Waves", Soil Dyn. Earthquake Eng., Vol. 13, pp. 365-375.
24. Luco, J.E. and de Barros, F.C.P. (1994a). "Dynamic Displacements and Stresses in the Vicinity of a Cylindrical Cavity Embedded in a Half-Space", Earthquake Eng. Str. Dyn., Vol. 23, pp. 321-340.
25. Luco, J.E. and de Barros, F.C.P. (1994b). "Seismic Response of a Cylindrical Shell Embedded in a Layered Viscoelastic Half-Space: I. Formulation", Earthquake Eng. Str. Dyn., Vol. 23, pp. 553-567.
26. Manoogian, M.E. (1992). "Scattering and Diffraction of Plane SH-Waves by Surface and Subsurface Topography of Arbitrary Shape", Ph.D. Dissertation, University of Southern California, Los Angeles, U.S.A.
27. Manoogian, M.E. (1995). "Scattering and Diffraction of SH-Waves by Sub-Surface Topography of Arbitrary Shape", Proc. Int. Conf. on Str. Dyn. Vib. and Noise Control, pp. 484-489.
28. Manoogian, M.E. (1996). "Scattering and Diffraction of SH-Waves by Non-Circular Surface and Sub-Surface Topography: Application of the Method of Weighted Residuals", Proc. Southeastern Conf.-Developments in Theoretical and Applied Mech., Vol. 18, pp. 66-79.
29. Manoogian, M.E. (1998a). "Scattering and Diffraction of SH-Waves near an Arbitrarily Shaped Canal", Proc. 12th Eng. Mech. Conf.–Eng. Mech.: A Force for the 21st Century, San Diego, California, USA, pp. 442-445.
30. Manoogian, M.E. (1998b). "Surface Motion above an Arbitrarily Shaped Tunnel due to SH-Waves", Proc. ASCE Goetech. Earthquake Eng. and Soil Dyn. Conf., Seattle, Washington, USA, pp. 754-765.
31. Manoogian, M.E. and Lee, V.W. (1995). "Scattering of SH-Waves by Arbitrary Surface Topography", Proc. Third Int. Conference on Recent Advances in Geotechnical Earthquake Eng. and Soil Dyn., Vol. 2, pp. 665-670.
32. Manoogian, M.E. and Lee, V.W. (1996). "Diffraction of SH-Waves by Sub-Surface Inclusions of Arbitrary Shape", ASCE Eng. Mech. Div., Vol. 122, pp. 122-129.
33. Pao, Y.H. and Mow, C.C. (1973). "Diffraction of Elastic Waves and Dynamic Stress Concentrations", Crane, Russak and Company, Inc., New York, U.S.A.
34. Sanchez-Sesma, F.J. (1987). "Site Effects on Strong Ground Motion", Soil Dyn. Earthquake Eng., Vol. 6, pp. 124-132.
35. Shah, A.H., Wong, K.C. and Datta, S.K. (1982). "Diffraction of Plane Elastic Waves in a Half-Space", Earthquake Eng. Struct. Dyn., Vol. 10, pp. 519-528.
36. Sherif, R. and Lee, V.W. (1997). "Diffraction around a Circular Alluvial Valley in a Wedge-Shaped Medium due to Plane SH-Waves", J. of European Association for Earthquake Eng., Vol. 10, pp. 21-28.
37. Trifunac, M.D. (1971). "Surface Motion of a Semi-Cylindrical Alluvial Valley for Incident Plane SH-Waves", Bull. Seism. Soc. Am., Vol 61, pp. 1755-1770.
38. Trifunac, M.D. (1973). "Scattering of Plane SH-Waves by a Semi-Cylindrical Canyon", Earthquake Eng. and Struct. Dyn., Vol. 1, pp. 267-281.
39. Wong, H.L. and Trifunac, M.D. (1974a). "Surface Motion of a Semi-Elliptical Alluvial Valley for Incident Plane Waves", Bull. Seism. Soc. Am., Vol. 64, pp. 1389-1408.
40. Wong, H.L. and Trifunac, M.D. (1974b). "Scattering of Plane SH-Waves by a Semi-Elliptical Canyon", Earthquake Eng. and Struct. Dyn., Vol. 3, pp. 157-169.
41. Wong, K.C., Shah, A.H. and Datta, S.K. (1985). "Diffraction of Elastic Waves in a Half-Space: II. Analytical and Numerical Solutions", Bull. Seism. Soc. Am., Vol. 75, pp. 69-92.
42. Yuan, X. and Liao, Z.P. (1994). "Scattering of Plane SH-Waves by a Cylindrical Canyon of Circular-Arc Cross-Section", Soil Dyn. Earthquake Eng., Vol. 13, pp. 407-412.
43. Yuan, X. and Liao, Z.P. (1995). "Scattering of Plane SH-Waves by a Cylindrical Alluvial Valley of Circular-Arc Cross-Section", Earthquake Eng. Struct. Dyn., Vol. 24, pp. 1303-1313.
44. Yuan, X. and Men, F. (1992). "Scattering of Plane SH Waves by a Semi-Cylindrical Hill", Earthquake Eng. Struct. Dyn., Vol. 21, pp. 1091-1098.